



## Science and Technology of Materials, Interfaces, and Processing

### Topical Areas

2D Materials  
Biomaterials  
Environmental S&T  
Magnetic Materials  
Manufacturing S&T  
Materials Characterization  
Materials Processing  
MEMS  
Microelectronic Materials  
Nanoscale S&T  
Plasma S&T  
Quantum Science  
Spectroscopic Ellipsometry  
Surface Engineering  
Surface Science  
Thin Films  
Vacuum Technology

### Contacts

Chief Operating Officer  
212-248-0200, ext. 222

Exhibition  
212-248-0200, ext. 229

Finance  
212-248-0200, ext. 224

Marketing/Meetings  
530-896-0477

Member Services  
212-248-0200, 221

Publications  
919-361-2787

Short Courses  
530-896-0477

Web/IT  
212-248-0200, ext. 223

### Officers

President-  
David P. Adams

President-Elect-  
Bridget R. Rogers

Past-  
President-  
Michael D. Williams

Clerk-  
David Surman

Treasurer-  
Gregory J. Exarhos

Directors-  
Ashleigh E. Baber  
Erica A. Douglas  
Robert K. Grubbs  
Caitlin Howell  
R. Mohan Sankaran  
Virginia "Ginger" Wheeler

AVS  
125 Maiden Lane, 15B  
New York NY 10038

Phone: 212-248-0200  
Fax: 212-248-0245  
E-mail: avsnyc@avs.org  
Web: www.avs.org

## 2024 Fall Meeting Hudson Mohawk AVS Chapter Thursday, October 17, 2024 3:30 – 7:30 PM

University at Albany  
ETEC building, Room B010  
1220 Washington Avenue, Albany, NY 12226

### Meeting Agenda

3:30 - 3:50 Reception (*coffee and cookies served*)

3:50 - 4:00 Welcoming Remarks

### Keynote Presentation

4:00 - 4:30 *Exploring Topological Conductors for Post-Cu Interconnects*  
**Dr. Ching-Tzu Chen** (IBM T.J. Watson Research Center)

### Oral Presentations

4:30 - 4:50 *Investigation of Low Temperature Fluorine-Based Etching Of TaN With Selectivity To SiOCH Dielectric,*  
**Ivo V. Otto IV** (UAlbany)

4:50 - 5:10 *Electronic Structure, Secondary Electron Yields, And Chemical Transformations of Photoresist Materials,*  
**Dr. Sylvie Rangan** (Rutgers)

5:10 - 5:30 *Degradation of Organosilicon-Functionalized Surfaces During X-Ray Photoelectron Spectroscopy: An In-Depth Study,*  
**Anthony Valenti** (UAlbany)

5:30 - 7:00 **Poster Presentations** (*pizza and refreshments served*)

7:00 - 7:20 **Student Awards Ceremony**

## Poster Presentations

**P1. MANGANESE BORIDE AS POTENTIAL INTERCONNECT METAL**

Sanzida Rahman (Rensselaer Polytechnic Institute)

**P2. MEASUREMENT OF THE DYNAMIC RESPONSE OF MEMS CANTILEVERS**

Alvar Garza (University at Albany)

**P3. ANGLE-RESOLVED PHOTOLUMINESCENCE SPECTROSCOPY OF ERBIUM-IMPLANTED THIN-FILMS AND NANOPHOTONIC STRUCTURES**

Souryaya Dutta, Blair Garrett (University at Albany)

**P4. ENHANCING PLASMONIC PHOTODETECTORS: A STUDY ON THE FABRICATION AND OPTICAL BEHAVIOR OF NANOANTENNAS**

Maryam Ahmadi (University of Connecticut)

**P5. DEVELOPMENT OF QUANTUM DOT SCINTILLATOR WITH INTEGRATED PHOTODETECTOR FOR ENHANCED RADIATION DETECTION**

Gyana Biswal (University at Albany)

**P6.  $\text{CuAl}_2$  AS CONDUCTOR FOR HIGH-CONDUCTIVITY INTERCONNECTS**

Zahra Ahmadian (Rensselaer Polytechnic Institute)

## Driving Directions

The ETEC building is in the Harriman State Office Complex, which is adjacent to the University at Albany campus. The address of the ETEC building is ETEC, 1220 Washington Avenue, Albany, NY 12226. It is important that you include "ETEC" in your search if you are using a mapping program; otherwise, the search will send you to the state police barracks.

### *From UAlbany Campus:*

There is no direct street access to the ETEC building from the UAlbany campus. You must first drive to either Washington Avenue or Western Avenue and go east towards downtown Albany. Just after passing the UAlbany campus, there will be an entrance to the Harriman State Office Complex (State Office Buildings).

- If entering Campus Access Road from Washington Avenue, you will see the ETEC building on your left. After passing the building, you will take a U-turn to access the side of Campus Access Road that passes in front of the ETEC building. The parking lot is on the north side of the building.
- If entering Campus Access Road from Western Avenue, you will also need to take a U-turn so that you are driving towards the ETEC building, not away from it. Again, the parking lot is on the north side of the ETEC building.

### *From the **North**:*

Take the Northway (I-87) south to Exit 1E. Merge onto I-90 east (toward Albany/Boston). Then take Exit 3 (State Office Buildings), which will put you on Campus Access Road. After passing the ETEC building, you will take a U-turn to access the side of Campus Access Road that passes in front of the ETEC building.

### *From the **South**:*

Take the Thruway (I-87) north to Exit 24. Merge onto I-90 east (toward Albany/Boston). Then take Exit 3 (State Office Buildings), which will put you on Campus Access Road. After passing the ETEC building, you will take a U-turn to access the side of Campus Access Road that passes in front of the ETEC building.

### *From the **West**:*

Take the Thruway (I-87) east to Exit 24. Merge onto I-90 east (toward Albany/Boston). Then take Exit 3 (State Office Buildings), which will put you on Campus Access Road. After passing the ETEC building, you will take a U-turn to access the side of Campus Access Road that passes in front of the ETEC building.

### *From the **East**:*

Take the I-90 west to Exit 3 (State Office Buildings), which will put you on Campus Access Road. After passing the ETEC building, you will take a U-turn to access the side of Campus Access Road that passes in front of the ETEC building.

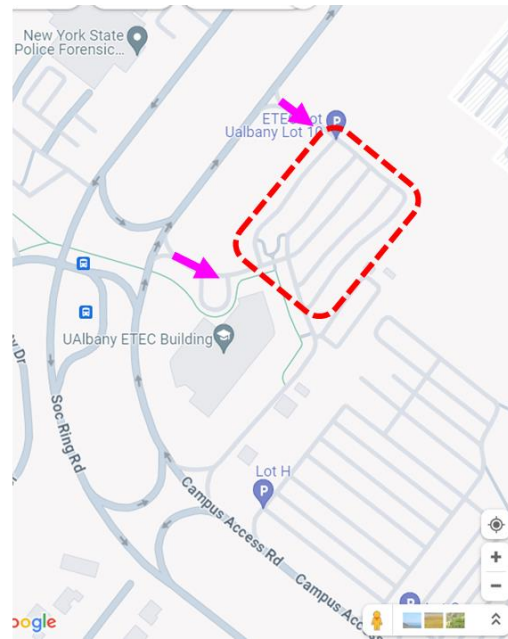
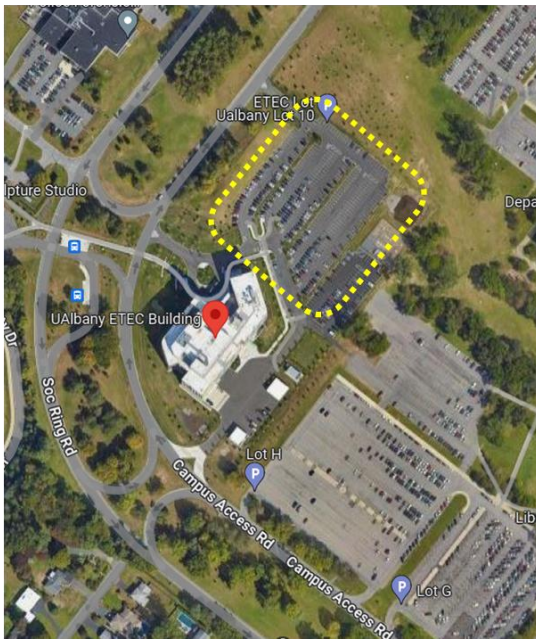
The address of the ETEC building is:  
**ETEC, 1220 Washington Avenue, Albany, NY 12226.**

It is important that you include “ETEC” in your search if you are using a mapping program; otherwise, the search will send you to the state police barracks.

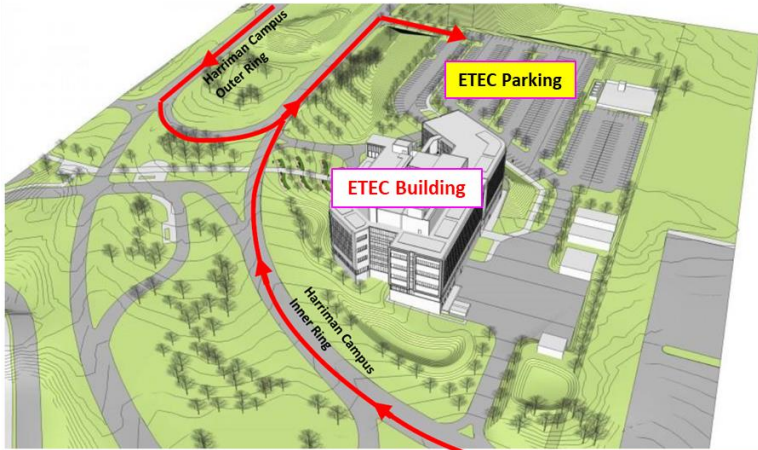
Print the parking permit and display it on your dashboard when parking in the ETEC lot. Otherwise you will have to pay at a UAlbany meter as a visitor.

HMAVS meeting location is in ETEC Room B010 (Basement level).

Enter ETEC Lot from Campus Access Road (inner ring road, one-way)  
(Purple Arrows)



From Washington Ave (North)



From Western Ave (US-20, South)

Keynote Presentation:

## **EXPLORING TOPOLOGICAL CONDUCTORS FOR POST-CU INTERCONNECTS**

Ching-Tzu Chen

*IBM Thomas J Watson Research Center  
Yorktown Heights, NY, United States*

[cchen3@us.ibm.com](mailto:cchen3@us.ibm.com)

Surface-state conduction in topological conductors yields unconventional resistivity scaling, such that resistivity decreases with reduced sample dimensions down to ~nm. This may provide a solution to the interconnect bottleneck in highly scaled integrated circuits. In this talk, we first review the theoretical electrical transport investigations of two prototypical topological semimetals, CoSi and NbAs, which provides insights into the resistivity scaling in topological conductors with and without defects. We then review the experimental data of CoSi thin films and wafer-scale nanowire devices down to ~5 nm scale. The magneto-transport measurements reveal coexisting high-mobility surface carriers with low-mobility bulk carriers. Most notably, we observe that room-temperature resistivity in nanoscale CoSi films can drop below the ideal bulk single-crystal limit, and the resistivity in highly textured CoSi nanowires reduces with the channel width. These proof-of-principle studies demonstrate the potential of topological conductors for post-Cu interconnect applications.

Oral Presentation:

## **INVESTIGATION OF LOW TEMPERATURE FLUORINE-BASED ETCHING OF TaN WITH SELECTIVITY TO SiOCH DIELECTRIC**

I. V. Otto IV, C. Vallée

*University at Albany, College of Nanotechnology, Science, and Engineering (CNSE),  
257 Fuller Road, Albany, NY 12203, USA*

[iotto@albany.edu](mailto:iotto@albany.edu)

The industry shift from SiO<sub>2</sub> and Al as the respective dielectric and conductor within the back-end-of-the-line (BEOL) interconnect superstructure to SiOCH low-κ dielectric and Cu improved key metrics such as RC delay, but had inherent integration challenges, one of which was Cu diffusion into the SiOCH film. The solution was the use of diffusion barriers, which are required in current integration schemes to prevent Cu diffusion. TaN is a key diffusion barrier candidate because of strong dielectric adhesion and low in-plane resistivity properties at 2-3 nm thicknesses. Creation of the BEOL interconnect superstructure is completed in cycles to create each metal level, requiring the repeated selective removal of not only Cu, but the TaN diffusion barrier, selective to the SiOCH.

SiOCH films attain dielectric constant values of between 2-3 by incorporating non-polar bonds (Si-CH<sub>3</sub>) and pores into their structure, making SiOCH sensitive to abrasive processes like CMP and physical, ion-assisted etching. Radical-dominated, fluorine etching of TaN with respect to SiOCH also comes with challenges because of the high volatility of SiF<sub>2</sub>, SiF<sub>4</sub>, and CF<sub>x</sub> SiOCH etch byproducts. We have previously explored methods to accomplish radical fluorine etching of TaN with selectivity to SiOCH as an alternative landing process on the SiOCH, for BEOL integration. Selective deposition of an SiOF film on the SiOCH film compared to the TaN, while etching the TaN, allowed the selective etching of TaN with respect to SiOCH. In this work, we explore the use of radical NF<sub>3</sub>/SiF<sub>4</sub> discharges, without O<sub>2</sub> addition (1), at sub-zero sample temperatures ranging from -45 °C to 0 °C (2). In this investigation, we seek to reduce the possibility of SiOCH damage by (1) removal of radical and atomic O interaction with the SiOCH film and (2) reduce the diffusion path for F to limit F diffusion through any SiF<sub>x</sub> deposition on the SiOCH, and to limit F diffusion within the SiOCH structure itself. We also explore selective removal of any remaining deposition on the SiOCH surface post-processing using plasma-free cleaning to confirm SiOCH integrity. *Ex-situ* spectroscopic ellipsometry is utilized to characterize film thickness changes after processing in addition to characterization of changes in film refractive index. *Ex-situ* X-ray photoelectron spectroscopy is used to probe the sample surface to characterize surface film properties, while *ex-situ* Fourier-transform infrared spectroscopy is used to analyze bulk SiOCH changes in the SiOCH bonding structure. Though this multi-modal investigation, we gain insight in the mitigation of SiOCH damage using an O<sub>2</sub>-free, low temperature process to selectively remove TaN.

*Graduate Student*

Oral Presentation:

**ELECTRONIC STRUCTURE, SECONDARY ELECTRON YIELDS, AND CHEMICAL TRANSFORMATIONS OF PHOTORESIST MATERIALS**

Sylvie Rangan and Robert A. Bartynski

*Department of Physics and Astronomy and Laboratory for Surface Modification  
Rutgers University, 136 Frelinghuysen Road, Piscataway, NJ 08854*

[rangan@physics.rutgers.edu](mailto:rangan@physics.rutgers.edu)

Future patterning strategies rely on High-NA EUV lithography, to achieve next generation dimensions of logic chips, with resolution requirements nearing 1 nm. At this scale, each step of the photoresist chemical transformation upon EUV exposure needs to be thoroughly understood, from the generation of secondary electrons by EUV photons, to molecular bond rearrangement upon resist exposure.

As chemical transformations are triggered by low energy electrons, it is crucial to understand and quantify electron energy loss channels in such materials as well as resulting secondary electron yields, as a function of the chemical environment. Additionally, proximity effects with underlayers may become increasingly important with resist film thickness reduction.

We have developed a unique platform able to correlate the yield of secondary electrons generated from incident electrons to the electronic structure and chemical properties of photoresist materials. Surface properties are assessed using x-ray and UV-photoemission spectroscopies, electron energy loss spectroscopy and work function measurements, and are interpreted in the light of ab-initio calculations of the electronic structure.

Two case-studies are considered. First, we study a set of four chemically amplified resist materials, as well as their individual components, using photoemission spectroscopies, electron energy loss spectroscopy and electronic structure calculations. Processes such as chemical transformations, phase segregation and electron energy loss channels are explored as a function of chemical composition. In a second example, we follow the chemical transformation of a polymethyl methacrylate film exposed to electrons using similar spectroscopic methods and additionally correlate the film's alteration to secondary electron yield evolution.



Oral Presentation:

## **DEGRADATION OF ORGANOSILICON-FUNCTIONALIZED SURFACES DURING X-RAY PHOTOELECTRON SPECTROSCOPY: AN IN-DEPTH STUDY**

Anthony Valenti<sup>1</sup>, Kandabara Tapily<sup>2</sup>, Kai-Hung Yu<sup>2</sup>, Steve Consiglio<sup>2</sup>, Cory Wajda<sup>2</sup>, Robert Clark<sup>2</sup>, Gert Leusink<sup>2</sup>, Christophe Vallée<sup>1</sup>, and Carl A. Ventrice, Jr.<sup>1</sup>

<sup>1</sup>*Department of Nanoscale Science and Engineering, University at Albany - SUNY*

<sup>2</sup>*TEL Technology Center, America, LLC*

[ajvalenti@albany.edu](mailto:ajvalenti@albany.edu)

Organosilicon precursors are often used to functionalize and passivate the SiO<sub>2</sub> regions of a substrate during area selective deposition. When using X-ray photoelectron spectroscopy (XPS) to characterize organosilicon-passivated SiO<sub>2</sub> surfaces, decomposition and/or desorption of the organosilicon functionalization can occur. The rate at which this degradation occurs depends on a variety of factors, such as the charge compensation technique used, the spot size of the X-ray beam, and the oxide thickness. In this study, these factors were evaluated for their influence on the degradation rate of the functionalized surface. Two different substrates were studied: 1,000 Å thermal oxide SiO<sub>2</sub>/Si(100) and 10 Å plasma oxide SiO<sub>2</sub>/Si(100). The surfaces of these substrates were first exposed to water vapor to hydroxylate the surface, followed by exposure to the organosilicon precursor *N*-(trimethylsilyl)dimethylamine (TMSDMA) to form a trimethylsilyl surface termination. Angle-resolved XPS analysis was performed on each sample type using either no charge compensation, electron beam compensation, ion beam compensation, or dual electron/ion beam compensation. The relative coverage of the trimethylsilyl-functionalization on the oxides surfaces were assessed by measuring the intensity of the O-Si(CH<sub>3</sub>)<sub>3</sub> signal in the XPS Si-2p region and by performing water contact angle measurements to determine the change in hydrophobicity of the surfaces. This investigation found that the degradation rate during XPS measurement for the samples with the 1,000 Å oxide was similar for all charge compensation techniques, including no compensation. On the other hand, the 10 Å oxide samples had a much lower degradation rate, except when ion beam compensation or dual beam compensation was used during the XPS measurements. The mechanisms for the differences in degradation rates of samples will be discussed in detail in this presentation.

*Graduate Student*



Oral Presentation:

## **TOWARD SCALABLE TELECOM SINGLE-PHOTON EMITTERS FOR QUANTUM PHOTONICS**

Alex E. Kaloyeros, Spyros Gallis

*College of Nanotechnology, Science, and Engineering (CNSE)  
SUNY University at Albany (SUNY Albany)  
Albany, NY 12203, USA*

[akaloyeros2@albany.edu](mailto:akaloyeros2@albany.edu)

The most efficient and scalable method for generating and detecting quantum information involves creating an integrated photonic platform that hosts a variety of compact on-chip quantum devices. Single-photon emitters (SPEs) associated with point defects and ions in semiconductors are currently seen as vital resources for many quantum photonic integrated circuit (PIC) applications. A key challenge in scaling SPEs from lab environments to long-distance fiber-based quantum networks is developing SPEs that operate in the near-infrared (NIR) telecom O to C wavelength range, which aligns with low propagation loss in fiber communication channels. The scalability of SPEs is hindered by limited material platforms, strict fabrication and operational temperature requirements (e.g.,  $\geq 77\text{K}$ , room temperature), and the random nature of current telecom SPE emitters, which complicate their fabrication and efficient coupling to other photonic devices and PIC chips. Furthermore, the absence of electrically driven SPEs in the telecom regime presents significant obstacles to developing telecom quantum LEDs (QLEDs). These critical scientific and technological challenges have yet to be addressed on a single platform, highlighting the complexity and importance of ongoing research to develop future scalable and compact quantum devices at telecom wavelengths. In this context, we present nanophotonic structures composed of arrays of silicon carbide (SiC) nanowires (NWs) and nanopillars (NPs) based on a novel and fabrication-compatible nanofabrication process. These structures enable the precise placement of erbium ( $\text{Er}^{3+}$ ) ions with state-of-the-art accuracy of  $\sim 10\text{ nm}$  and allow for the engineering of the optical properties of  $\text{Er}^{3+}$  ions. The structures exhibit high  $\text{Er}^{3+}$  photoluminescence (PL) excitation and emission efficiency at  $1.54\ \mu\text{m}$ , with near-radiative-limited lifetimes and an absorption cross-section ( $\sim 2 \times 10^{-18}\ \text{cm}^2$ ) that is two orders of magnitude larger than typical values in rare-earth-doped quantum materials. Additionally, the NWs facilitate polarized  $\text{Er}^{3+}$  emission, an important property for efficient coupling to optical cavities in quantum photonics applications. To this end, we simulate preliminary plasmonic cavity designs for Purcell enhancement of the  $1.54\ \mu\text{m}$  Er emission. Finally, we demonstrate a controlled approach to control the number of Er ions utilizing precise control over nanostructure geometry and implantation engineering, towards achieving the isolation of a single Er emitter.

*Graduate Student*

Poster Presentation:

## **MANGANESE BORIDE AS POTENTIAL INTERCONNECT METAL**

Sanzida Rahman and Daniel Gall

*Department of Materials Science and Engineering,  
Rensselaer Polytechnic Institute, Troy, NY 12180, USA*

[rahmas4@rpi.edu](mailto:rahmas4@rpi.edu)

Mn<sub>2</sub>B thin films are deposited by combined d.c. and r.f. co-sputtering from Mn and B targets in order to explore the potential of this new conductor as interconnect material. Mn<sub>2</sub>B belongs to a group of transition metal borides which have been predicted to be promising directional conductors for scaled interconnects, with a predicted conductivity in the limit of narrow wires that outperforms Cu by ~2x for the [001] crystalline direction of Mn<sub>2</sub>B. This study explores the deposition conditions for Mn<sub>2</sub>B films on Al<sub>2</sub>O<sub>3</sub>(0001), Al<sub>2</sub>O<sub>3</sub>( $\bar{1}\bar{1}20$ ) and Al<sub>2</sub>O<sub>3</sub>( $1\bar{1}02$ ) substrates as a function of temperature  $T_s = 400-800$  °C and relative power  $P_{Mn}$  and  $P_B$  to the Mn and B targets, with the goal to achieve phase-pure, stoichiometric Mn<sub>2</sub>B with a single orientation such that transport along [001] can be measured. X-ray diffraction (XRD) and energy dispersive spectroscopy (EDS) analyses indicate that the composition is a function of both  $T_s$  and the power to the Mn target, controlling the evaporation rate from the substrate and the deposition flux, respectively.  $T_s = 400$  °C leads to a low crystalline quality and  $T_s = 800$  °C causes dewetting and discontinuous films. Optimal deposition conditions include  $T_s = 700$  °C and 30 W dc and 100 W rf power applied to the Mn and B sources, respectively, resulting in polycrystalline Mn<sub>2</sub>B films on Al<sub>2</sub>O<sub>3</sub>(0001) and Al<sub>2</sub>O<sub>3</sub>( $\bar{1}\bar{1}20$ ) substrates with minimal impurity phases. Successful growth of epitaxial Mn<sub>2</sub>B(100) layers with a single orientation is achieved on Al<sub>2</sub>O<sub>3</sub>( $1\bar{1}02$ ) at 700 °C with  $P_{Mn} = 30$  or 40 W. However, XRD analyses indicate that the former contains grains of MnB and the latter Mn impurity phases. The epitaxy is confirmed by a 1.4° full-width at half-maximum (FWHM) of the  $\omega$ -rocking curve in combination with  $\varphi$ -scans indicating Mn<sub>2</sub>B(100) || Al<sub>2</sub>O<sub>3</sub>( $1\bar{1}02$ ) and Mn<sub>2</sub>B[010] || Al<sub>2</sub>O<sub>3</sub>[ $\bar{1}101$ ]. The next steps involve growing phase pure epitaxial Mn<sub>2</sub>B(100) layers and quantifying their resistivity size effect.

*Graduate Student*

Poster Presentation:

## **MEASUREMENT OF THE DYNAMIC RESPONSE OF MEMS CANTILEVERS**

Alvar Garza<sup>1</sup>, Luke Zink<sup>2</sup>, Anthony Valenti<sup>1</sup>, Matthew Strohmayer<sup>3</sup>, Joleyn Brewer<sup>3</sup>,  
Christopher Nassar<sup>3</sup>, Christopher Keimel<sup>3</sup>, and Carl A. Ventrice, Jr.<sup>1</sup>

<sup>1</sup>*Dept. of Nanoscale Science & Engineering, University at Albany, Albany, NY*

<sup>2</sup>*Department of Physics, Binghamton University, Vestal, NY*

<sup>3</sup>*Menlo Micro, Inc., Albany, NY*

[agarza@albany.edu](mailto:agarza@albany.edu)

Microelectromechanical systems (MEMS) are micron scale devices with moving parts. In particular, Menlo Micro produces radio frequency MEMS-based switches that have higher performance than conventional semiconductor-based switches. The MEMS switches use an electrostatically controlled cantilever that is made from a Au-Ni alloy. The electrical contacts of the switch are coated with ruthenium because of its resistance to oxidation at elevated temperatures. In addition, the most stable stoichiometry of ruthenium oxide is RuO<sub>2</sub>, which is an electrically conductive oxide. The MEMS devices are encapsulated in a predominately N<sub>2</sub> gas. During operation, it is important that the cantilever does not strike the contact at a velocity that might damage the protective RuO<sub>2</sub> overlayer. The goal of this project was to experimentally determine the resonant frequency and damping coefficient of the cantilever under different gas environments. A high vacuum chamber was modified to allow the insertion of a MEMS test module and the introduction of either N<sub>2</sub>, compressed dry air, or Ar into the chamber at various pressures. Our measurements showed that Ar provided the largest damping ratio. In addition, measurements were made of each cantilever's dimensions. The thicker cantilevers had the highest resonant frequencies.

*Undergraduate Student*

Poster Presentation:

**ANGLE-RESOLVED PHOTOLUMINESCENCE SPECTROSCOPY OF ERBIUM-IMPLANTED THIN-FILMS AND NANOPHOTONIC STRUCTURES**

Souryaya Dutta, Blair Garrett, Kevin Reyes, Prabha Prasad Nair, Alex E. Kaloyeros, and Spyros Gallis

*University at Albany, College of Nanotechnology, Science and Engineering (CNSE),  
Department of Nanoscale Science and Engineering*

[btgarrett@albany.edu](mailto:btgarrett@albany.edu)

In recent years, erbium-doped materials have attracted considerable attention as platforms for emerging telecom quantum information and integrated photonic technologies, primarily due to the key electronic transition of  $\text{Er}^{3+}$  around 1532 nm. Controlling the directionality and polarization of light emission from these materials and associated nanophotonic structures is critical for advancing efficient photonic, optoelectronic, and quantum optical devices. In this research, we applied fundamental physics and engineering principles to develop an experimental system capable of performing angle-resolved photoluminescence (PL) studies on erbium-implanted thin films (e.g., silicon carbide and lithium niobate) and nanophotonic structures. This system, designed to control both excitation and emission angles, enables angle-resolved PL measurements across the visible and near-infrared spectra. Leveraging this capability, we systematically studied the angle-resolved PL of erbium-doped thin films. Additionally, we established a clear relationship between the laser excitation angle and the angular distribution of Er PL emission, corroborating these experimental results with finite-difference time-domain (FDTD) simulations. Our findings demonstrate that angle-resolved PL microscopy can yield valuable insights into the emission characteristics of films and nanophotonic structures, which are crucial for the development of integrated photonic circuits.

Poster Presentation:

## **ENHANCING PLASMONIC PHOTODETECTORS: A STUDY ON THE FABRICATION AND OPTICAL BEHAVIOR OF NANOANTENNAS**

Maryam Ahmadi, John Grasso, and Brian G. Willis

*Department of Materials Science and Engineering,  
Department of Chemical and Biomolecular Engineering  
University of Connecticut, Storrs, CT*

[maryam.ahmadi@uconn.edu](mailto:maryam.ahmadi@uconn.edu)

The development of plasmonic nanoantennas has gained significant attention in recent years due to their unique ability to collect and focus light into nanoscale volumes. Nanoantennas, typically made from noble metals such as gold, copper, or silver, exhibit localized surface plasmon resonances (LSPRs) that enhance electromagnetic fields at the nanoscale. These resonances are sensitive to the size, thickness, geometric design, composition, and local environment of the nanoantennas. Potential applications include sensing, imaging, photocatalysis and energy harvesting.

In this work, we evaluate the top-down lithography methods such as electron beam lithography and photolithography to fabricate electrically interconnected nanoantennas on glass substrates. We utilize atomic layer deposition (ALD) to deposit thin film of aluminum oxide ( $\text{Al}_2\text{O}_3$ ) and titanium dioxide ( $\text{TiO}_2$ ) into PMMA photoresist-patterned surfaces to form photodetectors. We discuss deposition temperature, deposited thickness, and window size effects on ALD applied to e-beam patterned PMMA.

We employ simulation methods such as finite-difference time-domain (FDTD) to model the optical responses of the nanoantennas. The simulated results are then compared with the experimental data from the fabricated samples to validate our findings. The optical behavior of the fabricated features is characterized using spectroscopy techniques, optical extinction measurements. The results demonstrate a strong dependence of LSPR on the geometrical parameters of the nanoantennas, such as shape, size, and lattice spacing. We also measure the photocurrent generated by the nanoantennas under illumination, demonstrating their effectiveness in converting light into electrical signals. Moreover, we assess the potential of these nanoantennas to enhance light-matter interactions for applications in sensing and energy conversion.

*Graduate Student*

Poster Presentation:

**DEVELOPMENT OF QUANTUM DOT SCINTILLATOR WITH INTEGRATED PHOTODETECTOR FOR ENHANCED RADIATION DETECTION**

Gyana Biswal<sup>1</sup>, Tushar Mahajan<sup>1</sup>, Michael Yakimov<sup>1</sup>, Vadim Tokranov<sup>1</sup>, Michael Hedges<sup>2</sup>, Pavel Murat<sup>2</sup>, and Serge Oktyabrsky<sup>1</sup>

<sup>1</sup> *University at Albany- SUNY, Albany, NY, USA*

<sup>2</sup> *Fermi National Accelerator Laboratory, Batavia, IL, USA*

[gbiswal@albany.edu](mailto:gbiswal@albany.edu)

High-speed, high-efficiency radiation detectors are essential for a wide range of applications, such as medical imaging, high energy physics experiments, and homeland security. Here we have developed a novel semiconductor-based scintillation detector consisting self-assembled epitaxial InAs quantum dots (QDs) embedded into a GaAs matrix. The semiconductor heterostructure was grown by Molecular beam epitaxy (MBE). The detector consists of a 25  $\mu\text{m}$  thick scintillator released from the substrate with a monolithically integrated InGaAs p-i-n photodiode (PD) for improved optical coupling. Technology for a thin layer transfer and bonding is developed for low-parasitics integration of the detector with front-end electronics. Measurements of responses from  $^{241}\text{Am}$  alpha particles demonstrate collected charge in the range of 30- 50 photoelectrons per 1 keV of the deposited energy, or  $\sim 13\text{-}20\%$  of the theoretically achievable light yield of 240 el./keV in GaAs. The scintillation response shows an extremely fast 0.3-0.6 ns decay constant and about 40-70 ps time resolution for alpha particles, limited by the system noise. Experiments conducted in a vacuum are used to evaluate the detector's energy resolution limits. The combined decay time and light yield make the InAs/GaAs QD heterostructures the fastest high-yield scintillation material reported.

*Graduate Student*

## CuAl<sub>2</sub> AS CONDUCTOR FOR HIGH-CONDUCTIVITY INTERCONNECTS

Zahra Ahmadian<sup>1</sup>, Ching-Tzu Chen<sup>2</sup>, Atharv Jog<sup>3</sup>, Daniel Gall<sup>1</sup>

<sup>1</sup> *Materials Science and Engineering, Rensselaer Polytechnic Institute, Troy, 12180,*

<sup>2</sup> *Thomas J Watson Research Center, IBM Research, Yorktown Heights, 10598*

<sup>3</sup> *Advanced Logic Technology, IBM Research, Albany, 12203*

[Ahmadz2@rpi.edu](mailto:Ahmadz2@rpi.edu)

CuAl<sub>2</sub> is explored as possible Cu replacement for narrow high-conductivity interconnects, focusing on the possibility of liner/barrier-free CuAl<sub>2</sub> metallization. Epitaxial 70-300 nm thick CuAl<sub>2</sub>(110) and CuAl<sub>2</sub>(001) films are deposited on MgO(001) substrates by co-sputtering from Cu and Al targets at  $T_s = 100-400$  °C. X-ray diffraction confirms single-phase tetragonal CuAl<sub>2</sub> with a preferred 110 or 001 orientation for  $T_s = 100$  or 300-400 °C, respectively. Figure 1 shows the x-ray diffraction (XRD) patterns for these films. For an Al/Cu ratio of 2.1, the XRD pattern displays a dominant CuAl<sub>2</sub> 110 peak with no other misoriented grains nor secondary phases. However, as the Al content increases, an additional Al 200 peak appears at  $2\theta = 44.75^\circ$ , indicating the presence of excess Al.

Resistivity measurements are performed at room temperature (295 K) and in liquid nitrogen (77 K). The room temperature resistivity varies between 9.4 and 10.9  $\mu\Omega\cdot\text{cm}$  for Al/Cu ratios between 1.8 and 2.1, with the lowest value of 9.4  $\mu\Omega\cdot\text{cm}$  for the stoichiometric Al/Cu ratio of 2.0. Increasing the Al/Cu ratio to 2.3 leads to a resistivity drop to 8.4  $\mu\Omega\cdot\text{cm}$  which is caused by the conductive Al impurity phase, consistent with XRD results.

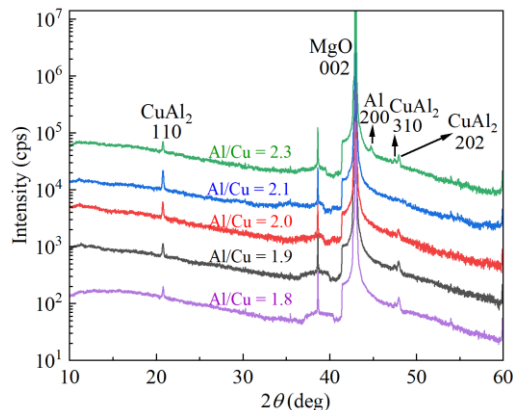


Figure 1:  $\theta$ - $2\theta$  x-ray diffraction patterns from CuAl<sub>2</sub>/MgO(001) layers with Al-to-Cu ratios Cu/Al = 1.8-2.3